

AFRL-ML-WP-TR-2003-4093

**HIGH-Q TUNABLE CAPACITORS AND
MULTI-WAY SWITCHES USING
MICROELECTROMECHANICAL
SYSTEMS (MEMS) FOR MILLIMETER-
WAVE APPLICATIONS**



**Dr. Y.C. Lee
Dr. K.C. Gupta
Dr. Victor M. Bright**

**The University of Colorado at Boulder
NSF Center for Advanced Manufacturing and Packaging
of Microwave, Optical and Digital Electronics
Boulder, CO 80309-0427**

DECEMBER 2002

Final Report for 28 August 1998 – 31 December 2002

Approved for public release; distribution is unlimited.

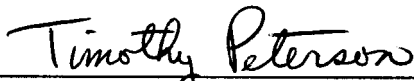
**MATERIALS AND MANUFACTURING DIRECTORATE
AIR FORCE RESEARCH LABORATORY
AIR FORCE MATERIEL COMMAND
WRIGHT-PATTERSON AIR FORCE BASE, OH 45433-7750**

NOTICE

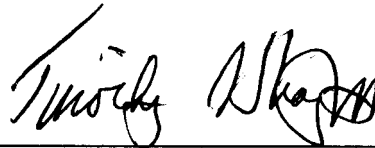
USING GOVERNMENT DRAWINGS, SPECIFICATIONS, OR OTHER DATA INCLUDED IN THIS DOCUMENT FOR ANY PURPOSE OTHER THAN GOVERNMENT PROCUREMENT DOES NOT IN ANY WAY OBLIGATE THE US GOVERNMENT. THE FACT THAT THE GOVERNMENT FORMULATED OR SUPPLIED THE DRAWINGS, SPECIFICATIONS, OR OTHER DATA DOES NOT LICENSE THE HOLDER OR ANY OTHER PERSON OR CORPORATION; OR CONVEY ANY RIGHTS OR PERMISSION TO MANUFACTURE, USE, OR SELL ANY PATENTED INVENTION THAT MAY RELATE TO THEM.

THIS REPORT IS RELEASABLE TO THE NATIONAL TECHNICAL INFORMATION SERVICE (NTIS). AT NTIS, IT WILL BE AVAILABLE TO THE GENERAL PUBLIC, INCLUDING FOREIGN NATIONS.

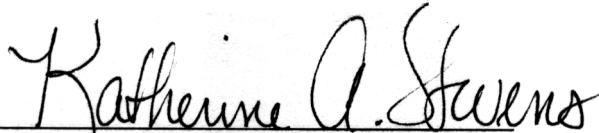
THIS TECHNICAL REPORT HAS BEEN REVIEWED AND IS APPROVED FOR PUBLICATION.



TIMOTHY L. PETERSON, Project Engineer
Sensor Materials Branch
Survivability & Sensor Materials Division



TIMOTHY J. STRANGE, III, Chief
Sensor Materials Branch
Survivability & Sensor Materials Division



KATHERINE A. STEVENS, Chief
Survivability & Sensor Materials Division
Materials & Manufacturing Directorate

Do not return copies of this report unless contractual obligations or notice on a specific document requires its return.

REPORT DOCUMENTATION PAGE				<i>Form Approved</i> <i>OMB No. 0704-0188</i>				
The public reporting burden for this collection of information is estimated to average 1 hour per response, including the time for reviewing instructions, searching existing data sources, gathering and maintaining the data needed, and completing and reviewing the collection of information. Send comments regarding this burden estimate or any other aspect of this collection of information, including suggestions for reducing this burden, to Department of Defense, Washington Headquarters Services, Directorate for Information Operations and Reports (0704-0188), 1215 Jefferson Davis Highway, Suite 1204, Arlington, VA 22202-4302. Respondents should be aware that notwithstanding any other provision of law, no person shall be subject to any penalty for failing to comply with a collection of information if it does not display a currently valid OMB control number. PLEASE DO NOT RETURN YOUR FORM TO THE ABOVE ADDRESS.								
1. REPORT DATE (DD-MM-YY) December 2002		2. REPORT TYPE Final		3. DATES COVERED (From - To) 08/28/1998 – 12/31/2002				
4. TITLE AND SUBTITLE HIGH-Q TUNABLE CAPACITORS AND MULTI-WAY SWITCHES USING MICROELECTROMECHANICAL SYSTEMS (MEMS) FOR MILLIMETER-WAVE APPLICATIONS				5a. CONTRACT NUMBER F33615-98-C-5429				
				5b. GRANT NUMBER				
				5c. PROGRAM ELEMENT NUMBER 62102F				
6. AUTHOR(S) Dr. Y.C. Lee Dr. K.C. Gupta Dr. Victor M. Bright				5d. PROJECT NUMBER 4348				
				5e. TASK NUMBER 71				
				5f. WORK UNIT NUMBER 16				
7. PERFORMING ORGANIZATION NAME(S) AND ADDRESS(ES) The University of Colorado at Boulder NSF Center for Advanced Manufacturing and Packaging of Microwave, Optical and Digital Electronics Boulder, CO 80309-0427				8. PERFORMING ORGANIZATION REPORT NUMBER				
9. SPONSORING/MONITORING AGENCY NAME(S) AND ADDRESS(ES) Materials and Manufacturing Directorate Air Force Research Laboratory Air Force Materiel Command Wright-Patterson AFB, OH 45433-7750				10. SPONSORING/MONITORING AGENCY ACRONYM(S) AFRL/MLPS				
				11. SPONSORING/MONITORING AGENCY REPORT NUMBER(S) AFRL-ML-WP-TR-2003-4093				
12. DISTRIBUTION/AVAILABILITY STATEMENT Approved for public release; distribution is unlimited.								
13. SUPPLEMENTARY NOTES Report contains color.								
14. ABSTRACT The objective of this project was to design new, innovative microelectromechanical systems (MEMS) to create high-Q tunable capacitors and switches that were superior to the existing on/off switches. The concept was feasible; however, it was very challenging to design and/or process MEMS to meet specific requirements balancing mm-wave and electro-mechanical performance measures, such as quality factor (Q), capacitance range, switching complexity, dynamic response, and reliability. Therefore, we planned to conduct in-depth synthesis and analysis to develop representative, well-characterized, MEMS-based, high-Q turnable capacitors, switches, and their mm-wave modules. We have successfully demonstrated innovative RF MEMS switches and variable capacitors and the associated knowledge and technology. The devices and subsystems demonstrated have confirmed the great potential of RF MEMS. More importantly, the knowledge and technologies developed for the design, packaging, and reliability of RF MEMS will assist the industry to develop cost-effective, reliable RF MEMS to support the advancement of military systems. Five major accomplishments are summarized in this report.								
15. SUBJECT TERMS MEMS, high-Q tunable capacitors								
16. SECURITY CLASSIFICATION OF: <table border="1" style="width: 100%; border-collapse: collapse;"> <tr> <td style="width: 33%; padding: 2px;">a. REPORT Unclassified</td> <td style="width: 33%; padding: 2px;">b. ABSTRACT Unclassified</td> <td style="width: 33%; padding: 2px;">c. THIS PAGE Unclassified</td> </tr> </table>			a. REPORT Unclassified	b. ABSTRACT Unclassified	c. THIS PAGE Unclassified	17. LIMITATION OF ABSTRACT: SAR		18. NUMBER OF PAGES 32
a. REPORT Unclassified	b. ABSTRACT Unclassified	c. THIS PAGE Unclassified						
19a. NAME OF RESPONSIBLE PERSON (Monitor) Timothy L. Peterson 19b. TELEPHONE NUMBER (Include Area Code) (937) 255-4474 x3235								

Overall Project Objectives Proposed

This project was to design new, innovative microelectromechanical systems (MEMS) to create high-Q tunable capacitors and switches that were superior to the existing on/off switches. The concept was feasible; however, it was very challenge to design and/or process MEMS to meet specific requirements balancing mm-wave and electro-mechanical performance measures such as quality factor (Q), capacitance range, switching complexity, dynamic response and reliability. Therefore, we planned to conduct in-depth synthesis and analysis to develop representative, well-characterized, MEMS-based high-Q tunable capacitors, switches and their mm-wave modules. In addition, we were to establish a technology and knowledge base to transfer these new components into practical applications.

Summary

We have successfully demonstrated innovative RF MEMS switches and variable capacitors and the associated knowledge and technology. The results are well recognized by academic and industrial researchers, and their impact is growing everyday. The devices and subsystems demonstrated have confirmed the great potential of RF MEMS. More importantly, the knowledge and technologies developed for the design, packaging and reliability of RF MEMS will assist the industry to develop cost-effective, reliable RF MEMS to support the advancement of military systems. Five major accomplishments are to be summarized in this report:

I. Foundry-based RF MEMS Enabled by Flip-Chip Assembly: This has been the only technology ever reported that allowed the use of foundry-based silicon MEMS for microwave or millimeter-wave applications. Foundry fabrication is critical to assure the quality of the MEMS while reducing costs. II. Atomic Layer Deposition (ALD) for MEMS: A nano-scale multiplayer coated on MEMS by ALD has proven its potential to be the solution for MEMS reliability. This is the inorganic protective layer that will replace organic, self-aligned monolayer (SAM) being used by MEMS manufacturing in future. More importantly, ALD enables us to design a multiplayer dielectric layer with charge dissipation capability, which is critical to develop reliable RF MEMS. III. RF MEMS Prestressed-Beam Switch for Cryogenic Applications: This is a novel RF MEMS switch with the operation principle completely different from other MEMS switches'. Thermal mismatch is not a problem in this design; instead, it is used to make the RF connections. IV. Variable MEMS Capacitor for RF Applications: After generations of improvement, we have demonstrated the best variable MEMS capacitor ever reported, and we have the knowledge and technology to improve it. V. Reflection-type MEMS Variable-Capacitor Phase Shifters: This is the first phase shifter controlled by MEMS variable capacitors. It is compatible with planar patch antenna array.

New grants have been awarded from other DARPA programs, NASA and industrial partners. The knowledge and technology developed in this project have been transferred successfully to these RF MEMS improvement R&D activities for military and commercial applications.

Two papers received awards from international conferences. One U. S. patent application on ALD has been filed. Four keynote speeches have been presented in conferences. 20 papers have been published or accepted for publications. Five students fully or partially supported by the project received Ph.D.

I. Foundry-based RF MEMS Enabled by Flip-Chip Assembly

I.1 Summary

Foundry fabrication is important to manufacture high-quality, low-cost RF MEMS. But, today, all the MEMS foundry services are based on silicon substrate, which is not compatible with RF applications. We have developed a flip-chip with silicon removal technology that enabled us to transfer MEMS devices from the host silicon substrate to a new substrate, e.g. alumina, for RF circuits. According to our knowledge, this technology has been the only technology ever reported that allowed the use of foundry-based silicon MEMS for microwave or millimeter-wave applications. Corresponding to this technology, we have established a design method with a consideration of upside-down configuration. In addition, RF and mechanical design methods has been developed to assure excellent RF performance, which was demonstrated by many devices designed, fabricated, assembled and tested.

I.2 Foundry-fabricated MEMS

As shown in Figure I.1, within the first year, over 100 RF MEMS devices were designed, fabricated and tested using a MEMS foundry service offered by Cronos Integrated Microsystems (formerly known as MCNC MEMS Technology Division). Throughout the 4-year project period, many more devices have been developed using the same process. The foundry process is known as MUMPS (Multi-User MEMS Processes), which is the most popular foundry process for prototyping.

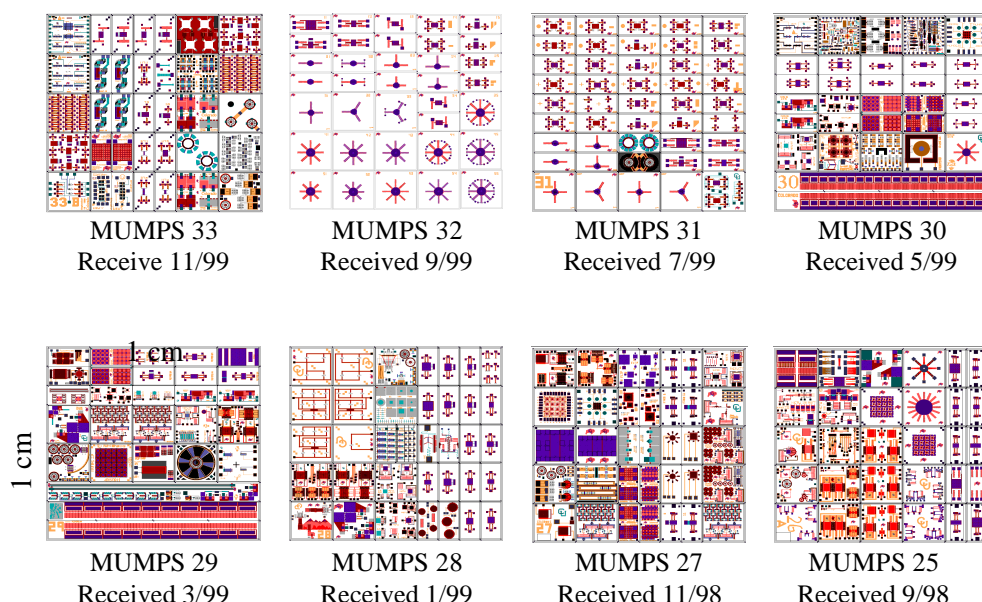


Figure I.1: Over 100 RF MEMS designed for MUMPS fabrication in Year-1

The MUMPS used low-resistivity silicon as the host substrates; therefore, we have developed a new flip-chip assembly with silicon removal process to transfer the MEMS to a new ceramics substrate. Referring to Figure I.2, After flip-chip bonding, HF removed SiO_2 sacrificial layers and a specific layer placed between the MEMS and the host silicon substrate. Figure I.3 shows a MEMS devices after transferring onto the ceramics substrate. Such a MEMS device's RF performance could be as good as any other RF MEMS devices directly fabricated on GaAs or ceramics. Using foundry service, however, we could study hundreds of MEMS devices with complex structures. Most of GaAs- or ceramics-based MEMS devices are very simple, e.g. on/off switches, because their fabrication infrastructure is very limited. Our team is the only team developing RF MEMS devices using the flip-chip assembly with silicon removal process. Such a technology enabled us to investigate many different devices quickly.

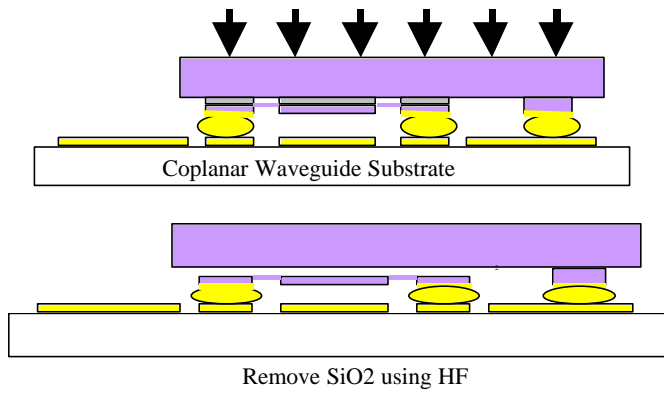


Figure I.2: Flip-chip assembly followed silicon removal for RF MEMS

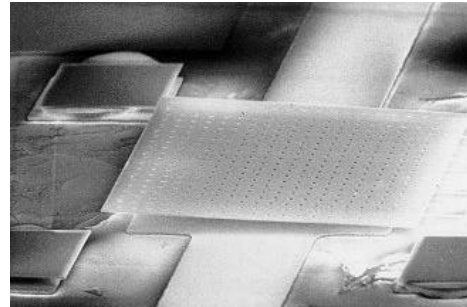


Figure I.3: MEMS device transferred onto a by new ceramics substrate

In addition, the flip-chip assembly technology offers hybrid integration potential. As shown in Figure I.4, the best strategy to implement RF MEMS is to integrate them with other RF circuits or components, e.g. superconductor filter circuits or ferroelectric tuning circuits.

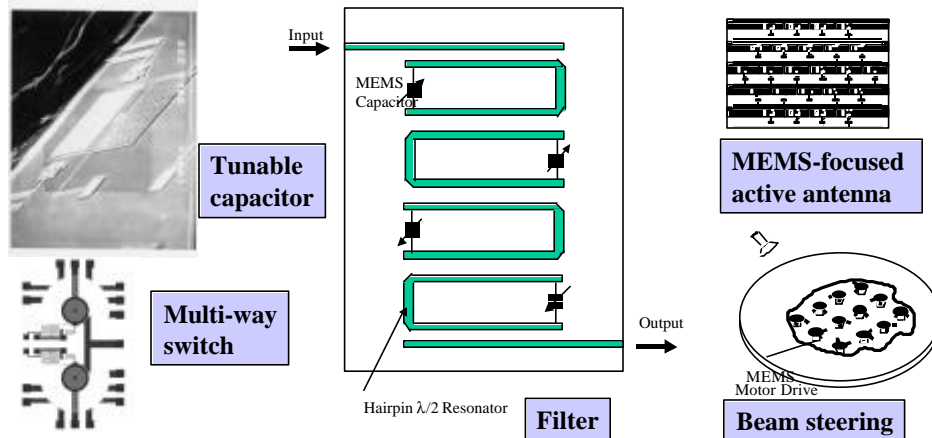


Figure I.4: Hybrid integration of MEMS with other RF circuits

I.3 Tunable capacitor using indirect thermal drive

The flip-chip assembly with silicon removal technology has been demonstrated by a MEMS-based variable capacitor with outstanding RF performance acceptable for millimeter-wave applications. Figure I.5 shows the capacitor driven by four vertical thermal actuators. The actuators moved the MEMS plate up-and-down to change the air gap between the MEMS and the signal line of a coplanar-waveguide (CPW). The air gap change resulted in a capacitance change with a ratio up to 2.7: 1. Air's dielectric loss was negligible; therefore, this MEMS-based capacitor achieved a very impressive quality factor (Q) that was about 300 at 0.1 pF and 10 GHz. In addition, as shown in Figure I.6-a, the capacitance showed no resonance and the equivalent resistance was less than 0.5Ω in the frequency range up to 40 GHz. According to our knowledge, the best MEMS capacitor's performance reported by other studies was $Q=62$ (2.11 pF and 1 GHz) with 6 GHz as the maximum operating frequency. Figure I.6-b shows Q-values normalized by having the same 0.1 pF and 10 GHz. Such normalization assumed the same equivalent resistance, which might not be true. However, it is a good approach to compare devices reported with different Q values at different capacitance and frequency ranges. Clearly indicated, our MEMS capacitor set a new record in Q-value. With this new MEMS device, we have successfully introduced MEMS into millimeter-wave applications.

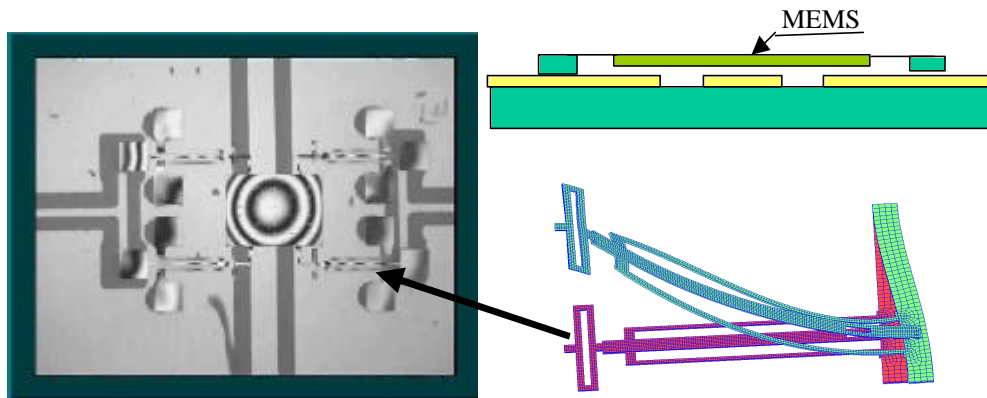


Figure I.5: MEMS-based variable capacitor driven by vertical thermal actuators

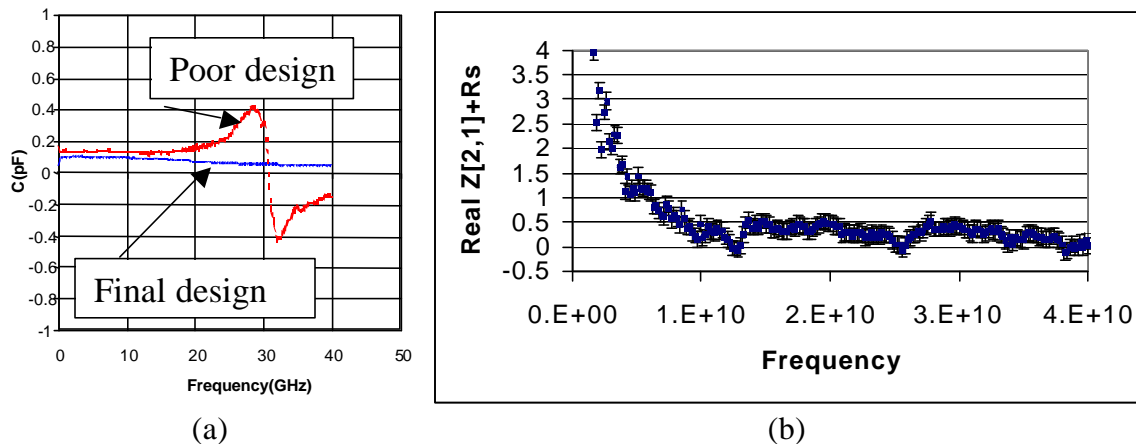


Figure I.6: Measured capacitance and resistance values up to 40 GHz

To achieved such impressive performance, we have solved three major problems:

RF design: It was critical to control the resonant frequency and the de-coupling between the actuators and the MEMS plate. With a poor inductance design, the MEMS could reach the undesirable resonance around 30 GHz (see Figure I.6-a). Changing the MEMS plate, the width of the actuators and the RF connection scheme solved this resonance problem. In addition, RF design was conducted to de-couple the actuator from the capacitance plate. As shown in Figure I.6-b, the actuator inductance became effective for de-coupling and reduced the resistance significantly when the frequency was above 10 GHz.

Assembly: The flip-chip assembly with the silicon removal technology was critical to transfer the MEMS to the ceramic substrate for excellent RF performance.

Actuator design: The vertical displacement of the actuator was driven by the thermal mismatch between the hot and the cold arms. However, when the cold arm was placed in the middle between the two hot arms, the cold arm's temperature could be higher than the corresponding hot arm . By placing the hot arm in the middle, we have achieved a consistent temperature differential for repeatable up-and-down plate movements (see Figure I.7).

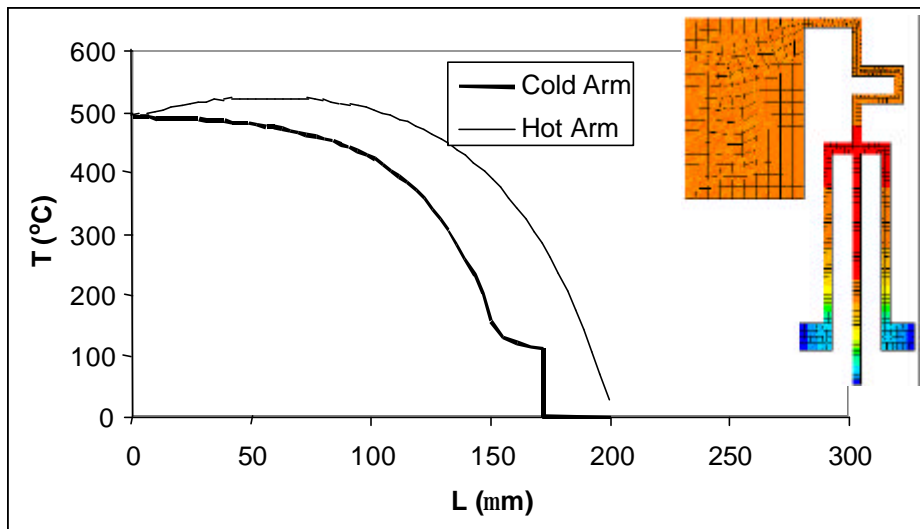


Figure I.7: Temperature distributions of an improved actuator with the hot arm in the middle

In addition to actuators, new designs have been derived to reduce the plate warpage for the tunable capacitors. Because of the thermal mismatch between the gold and the polysilicon layers, the plate warped. The warpage affected the performance of the capacitor consisting of two "parallel" plates. A new design was to interconnect gold cells to cover the entire plate. Each cell was small and would result in small thermal mismatch. For a flat plate with good RF performance, the "interconnections" of these cells are electrically good but mechanically weak. Unfortunately, due to unpredictable property

variations of thin film gold and polysilicon, the design simulation might not be accurate. We have to rely on experiments to choose the best design out of a group of designs with parametric variations.

Variable capacitors have been designed and studied. Figure I.8 shows a typical MEMS chip with these capacitors. In addition, different multi-way switches and electrostatic-driven variable capacitors have been developed and they are also shown in the same chip layout. The flip-chip assembly with silicon removal technology has been improved during the project period. It has been used for most of RF MEMS devices to be studied. Four notable demonstrations will be described in the following sections.

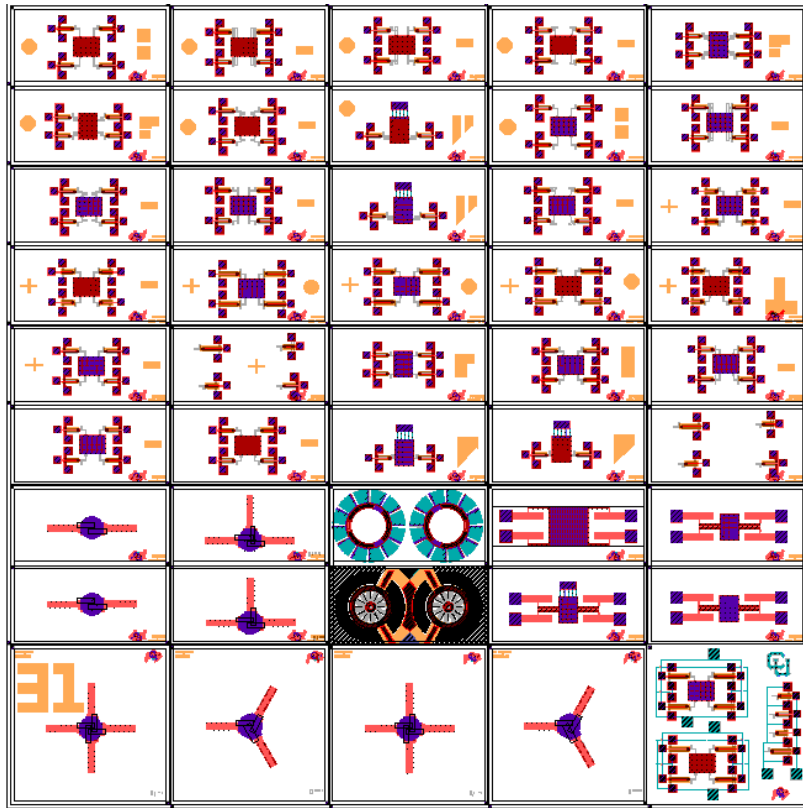


Figure I.8: A chip submitted for MUMPS fabrication with a group of tunable capacitors with parametric variations and with two-way and three-way switches

II. Atomic Layer Deposition (ALD) for MEMS

II.1 Summary

For electrostatically actuated MEMS devices, a novel fabrication approach of coating released MEMS devices with nanometer-thin films using atomic layer deposition (ALD) developed at the S. George Research Group at the University of Colorado at Boulder, has been shown to prevent an electric short when actuated. The ALD process is capable of depositing a variety of thin-film materials to protect MEMS devices from electrical breakdown, mechanical wear and stiction failure. ALD ensures conformal film coverage on all sides of a released MEMS device and can be performed at relatively low temperature of 177 °C, compared to CVD processes at 4-600 °C. The ALD film thickness can be precisely controlled at the atomic level as each reaction cycle deposits approximately one atomic monolayer. To demonstrate the concept of conformal layer deposition, ALD alumina (Al_2O_3) films were deposited onto released MEMS cantilever beams and the coated devices were subsequently analyzed using cross sectional scanning electron microscopy. Electrostatic testing of the coated MEMS cantilever beams revealed that the ALD Al_2O_3 films prevented electrical shorting and failure when the devices were activated beyond the pull-in voltage. For the RF-MEMS variable capacitors, the ALD alumina is used as a dielectric layer to prevent electrical shorting, and is essential to the performance and operation of the devices.

The nano-scale multiplayer coated on MEMS by ALD has a great potential to be the solution for MEMS reliability. This is the inorganic protective layer that will replace organic, self-aligned monolayer (SAM) being used by MEMS manufacturing in future. More importantly, ALD enables us to design a multiplayer dielectric layer with charge dissipation capability, which is critical to develop reliable RF MEMS.

II.2 Introduction

Micro-electromechanical Systems (MEMS) have in several applications proven excellent lifetime and reliability in terms of mechanical strength and material properties, but this has largely been the case for devices with individual silicon surfaces not in contact with each other or with harsh environments. Thus, a novel fabrication approach using atomic layer deposition (ALD) to coat and protect released MEMS devices have been investigated. The ALD process used on the MEMS devices is developed by the S. George Research Group at the University of Colorado at Boulder. ALD is a coating process capable of depositing ultra-thin, conformal films of a variety of materials with atomic-level thickness control. The ALD process relies on a binary reaction sequence of self-limiting chemical reactions with one atomic layer deposited during each cycle.

MEMS reliability may be improved by using conformal layers of material to prevent electrical shorting, improve wear resistance, prevent stiction or impart biocompatibility. A conformal layer of a dielectric material such as alumina (Al_2O_3) may prevent electrical shorting between conducting parts that come into contact. Thin, conformal coatings of hard materials such as Al_2O_3 or SiC should protect moving parts from wear thereby increasing the MEMS device lifetime. In addition, anti-stiction coatings comprised of

hydrocarbon or fluorocarbon monolayers may eliminate stiction in suspended MEMS structures. Adhesion caused by the build-up of static charge should be alleviated by depositing conducting coatings with controlled resistance. Finally, coating MEMS devices with biocompatible materials such as TiO_2 may allow the devices to operate in-vivo. All of these coating examples could potentially be realized using ALD thin film growth techniques.

Protective and anti-stiction surface coatings have previously been deposited on released MEMS structures using chemical vapor deposition (CVD) and self-assembling monolayer (SAM) techniques. There are several advantages of these coating techniques, but they possess some inherent limitations. SAM coatings have a maximum thickness of only one organic monolayer and consequently they have limited wear resistance. CVD processes require relatively high deposition temperatures and yield limited thickness control and conformality.

ALD offers a number of advantages when compared to the SAM and CVD coating processes. Perhaps the greatest advantage of the ALD process is the remarkable conformality of the deposited films. ALD films will cover all sides of a released MEMS device including bottom surfaces, such as underneath cantilever beams. This feature is illustrated in Figure II.1. As long as the gaps between the different components are larger than the ALD precursor molecules, the precursor gases will diffuse into the gaps and deposit a film. In addition, ALD allows precise thickness control because the film is deposited in a stepwise, layer-by-layer fashion.

Another advantage of ALD is that it can be performed at temperatures well below typical CVD temperatures. For instance, Al_2O_3 ALD has been demonstrated by the S. George Research Group at temperatures as low as 35 °C. However, the drawback of such a low temperature is that the coating process is very slow. Thus, a temperature of 177 °C is typically used to optimize the process. Yet, this temperature allows for the coating of composite devices comprised of different materials such as polysilicon and gold without damaging the device. Thermally sensitive polymer based MEMS and MEMS incorporated into integrated circuits could also be coated using low temperature ALD.

In general, for a coating to be a viable solution to the problems encountered in RF-MEMS devices, it should meet the following requirements:

- Electrical Conductivity - control of resistivity is desired to avoid charge accumulation as well as electrical shorting and isolation.
- Material Compatibility - Conformal, chemically stable, and compatible to materials commonly used in the surface micromachining process of MEMS.
- Mechanical Properties - must not interfere with the ability of the MEMS device to be mechanically actuated, yet be protective enough to allow large numbers of contact cycles.

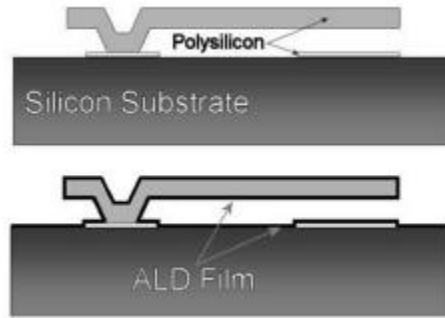


Figure II.1: Illustration of released cantilever beam and conformal ALD film growth.

II.3 Results

To illustrate the conformality of the ALD deposited alumina layer onto polysilicon devices, some of the cantilevers were broken with a probe tip such that a cross-sectional image could be obtained. Figure II.1A and B are FEG-SEM (Field Emission Gun Scanning Electron Microscope; which allows for imaging of insulated specimens without conductive coating) pictures illustrating the corner of a polysilicon beam before and after ALD coating. The 80-nm ALD deposited alumina layer can clearly be seen as it follows the contour of the cantilever beam both on top and sidewall as shown in Figure II.1B.

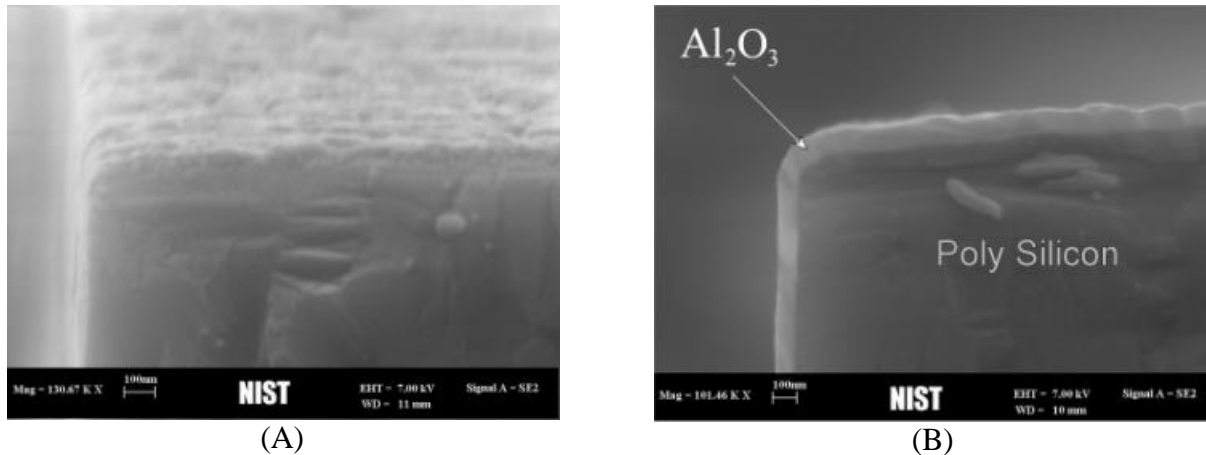


Figure II.1: (A) SEM close-up of uncoated sample. (B) SEM of cantilever beam coated with a 80-nm thick alumina layer. The picture clearly illustrates the conformability of the ALD film.

To further investigate the ALD coating, the samples coated with 60 nm of alumina were investigated using Focused Ion Beam (FIB) and Scanning Electron Microscopy (SEM) techniques. One of the cantilever beams was cut using the FIB and close-up pictures of the alumina layers were taken using SEM. The FIB cuts directly down through all the layers in the cantilever beam, electrode below, and silicon substrate. Using a polishing cut to remove any residue and overhang, one can see the individual layers and the cutout section will appear clearer. Figure II.3 provides a high-resolution close-up of the cutout section. Alumina is a dielectric and thus discharges electrons during SEM investigation and will

appear white. The white line on top on the poly-0 layer and underneath the polysilicon structure is the ALD-deposited alumina. The additional layer under the released top section is material re-deposition that occurs during FIB investigation.

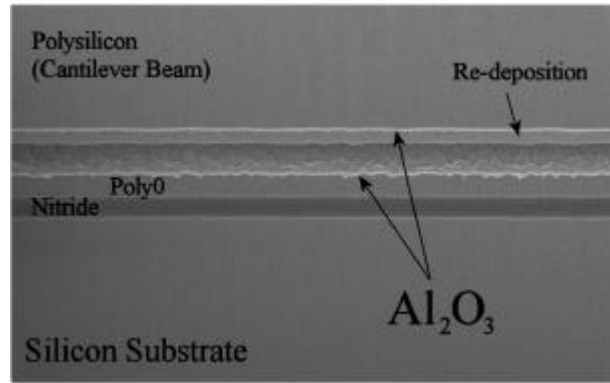


Figure II.2: SEM close-up of individual layers of the cantilever beam illustrating the polysilicon, air gap, ALD-coated alumina, and silicon substrate. The alumina layer can be seen as the thin white lines underneath the beam and on top of the poly-0 electrode.

Further testing revealed that ALD coating of electrostatically driven cantilever beams prevented shorting and failure when activated beyond pull-in voltage, and the cantilever beams could repeatedly be actuated beyond the snap-through voltage (more than 100,000 contact cycles without shorting observed during basic electrostatic tests for the 200 μm long beams). However, an increase in beam stiffness was observed, due to the added stiffness of the coating layer. Interferometric measurements of coated cantilever beams indicate an increase in radius of curvature for coated MEMS devices. This might imply an uneven coating thickness on top and underneath the cantilever beam. A change in beam stiffness can easily be accounted for by slight modifications in component design, whereas the increase in curvature could be eliminated by properly determining the optimal ALD reactant exposure-times thereby allowing the reactants to completely saturate the surface sites underneath suspended MEMS devices. For the RF-MEMS variable capacitors described within this thesis, the ALD alumina dielectric layer enables electrostatic actuation of the electrostatically-actuated capacitors without shorting. The actuation voltage for these devices also increased after ALD coating, but this is expected since the stiffness of the flexures in the MEMS device will increase when coated. This is generally tolerable since it can easily be compensated for by modification in design.

In addition to alumina coating using ALD, $\text{Al}_2\text{O}_3/\text{ZnO}$ multiplayer could be desposited. ZnO layer is conductive. When this layer is in the order of several angstroms, it becomes transparent to microwaves. As a result, we have a good technology to fabricate a composite dielectric layer that may dissipate charge accumulated while maintaining good dielectric characteristics. In addition, ALD-coating can go through post-treatment to make the surface hydrophobic, which is desirable to avoid moisture-induced reliability problem. We have received funding from DARPA Improvements Program to continue this study. ALD is now well recognized as one of the most promising technologies to solve MEMS reliability problems.

III. RF MEMS Prestressed-Beam Switch for Cryogenic Applications

III.1 Summary

RF MEMS switches operating at cryogenic temperature have not been reported so far. We have designed, fabricated and tested a novel RF MEMS switch operating at 77 K. This MEMS switch is composed of a switch plate suspended by two prestressed cantilever beams. These cantilever beams are made of two layers: 0.5 micron-thick gold and 1.5 micron-thick polysilicon layers. The thermal mismatch between the gold and polysilicon layers causes the cantilever beams to warp in the direction of the gold layer. At room and cryogenic temperatures, the deformed beams press the switch plate onto the CPW line. As a result, the switch plate is normally in contact with the CPW line in the absence of a bias voltage. This corresponds to the OFF-state in the shunt switch design. An actuation electrode is placed on the side of MEMS structure away from the CPW. The switch beams act as the other electrode. When a DC voltage is applied, the switch beam and plate moves away from the CPW structure. This corresponds to the ON-state for the shunt switch design. For low operating temperature design, mechanical and electrical models are constructed to predict the switch behavior. The pre-stressed beams, the switch plate and the coupling structures in between are designed with the help of the thermal-mechanical model in CoventorWare, in order to achieve large out-of-plane switch displacement and reliable surface contact at cryogenic temperatures. The optimal switch design shows the out-of-plane displacement of 30 microns for the 500 micron-long beam. For the electrical design, the effect of the bias electrode on the switch insertion loss is modeled and discussed. For design reported, the measured insertion loss is optimized to be less than 0.8 dB up to the 40 GHz. The difference of the insertion losses between the switch and the same length CPW line is less than 0.3 dB. The measured isolation values at both temperatures of 300 K and 60 K are both -12 dB at 20 GHz, showing the isolation is not affected by cryogenic temperature.

III.2 Introduction

There are several RF MEMS switches reported in literature. But there is no information available for their operation at cryogenic temperatures at this time. At University of Colorado, we have designed, fabricated and successfully tested a MEMS switch operating at 77 K. The design reported here employs a pre-stressed beam that presses against and provide a RF short-circuit (high capacitance) across a transmission line (coplanar waveguide configuration). When an actuation voltage is applied, the beam moves away from the RF transmission line, allowing signal to pass through and the switch is in ON state. On the other hand, the signal does not propagate across the switch location when no voltage is applied and the switch is shorting the line. This is the OFF state for the switch.

A. Initial Switch Configuration

We use MUMPs, a polysilicon-based foundry process, to prototype MEMS switches. The MEMS structure consists of multiple layers of polysilicon and a single layer of gold, separated from the silicon substrate by a sacrificial layer of silicon dioxide. After being dipped in HF acid, the sacrificial silicon oxide is etched and the MEMS structure is released. Then the MEMS chip is flip-chip bonded on the Alumina substrate. A cantilever beam consisting of polysilicon and gold layers functions as the moving

part of the switch assembly. A thin layer of silicon nitride isolates prestressed beam and bias electrode layer from low resistivity silicon substrate. Dimples on the polysilicon layer of pre-stressed beam and corresponding notches in the bias electrode layer prevent the beam from contacting the bias electrode. The cross section of the assembly is shown in Fig. III.1.

Because the gold layer is deposited at an elevated temperature during MUMPs fabrication, the beam curls up due to the residual thermal stress (Fig. III.2), like a bi-metal strip. This deformation is utilized to make the switch contact the RF line without any electrostatic force applied (we call it the down-state switch position throughout this paper). As seen in Fig. III.1, the upper polysilicon layer on the MEMS chip functions as the bias electrode. When a voltage is applied between the bias electrode and the switch beam, the electrostatic force pulls the free end of the beam upward and the switch moves to its up-state position.

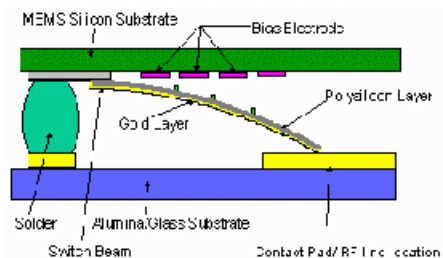


Fig. 1. Cross-section of the prestressed beam structure.

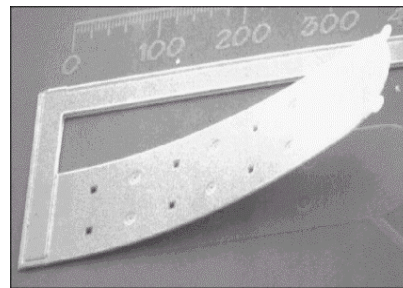


Fig. 2. SEM of a prestressed beam (Dimensions shown on the substrate are in microns).

B. Structural Design

The switch needs to be designed to address the issues related to the capacitive switching operation at cryogenic temperature. Mechanical design for this switch includes various issues that are described below.

- *Planarity of the contact plate and structural symmetry*

A separate rigid plate is designed for flat contact to obtain higher down-state capacitance. This plate is suspended by two flexible links connected to the two prestressed beams at two sides. The switch structure is made to be symmetric. Fig. III.3 (a) and (b) only shows one half of the switch including one beam and half of the switch plate. The whole structure is symmetric with respect to the dotted line in Fig. III.3 (a) and (b).

Details of this flat contact plate are shown in Fig. III.3. In the contact plate area, the polysilicon layer is made thicker and the gold layer is sliced into patches to reduce the deformation due to thermal warping. Some of the designs have the gold removed to eliminate the thermal mismatch between the polysilicon and gold on the plate.

- *Flexible connections*

When the flexible links (in Fig. III.3(a) and (b)) become stiff, the plate cannot have large displacement. If the links are made too thin (to increase flexibility), they are more likely to break and the lifetime of the switch will be reduced. Therefore an optimum design of links is needed. A number of these flexible link geometries have been modeled using 3-D finite-element modeler ConventorWare to arrive at the optimum design.

- *Lateral warpage of the beam*

As shown in Fig. III.3(a), the gold layer on the beam is also sliced in three stripes along the length direction in order to avoid the undesired lateral (along the width of the beam) deformation.

III.3 Measurements

A. D.C. Connection Resistance

The D.C. connection resistance is also measured continuously with respect to the temperature change (shown in Fig. III.4). This figure is a plot of temperature and D.C. resistance measured as functions of time when the chamber temperature is increased from 77 K to 300 K. R is the resistance between the lower pad of the solder bump (the upper solder pad being connected to the switch beam) and the contact pad when the switch beam is in pull-down state. It includes the resistance between contact pad and switch beam tip, resistance of gold/polysilicon layer on the beam, resistance of solder bump, metalization between solder pad and probe pad, and metalization between contact pad and probe pad. We note that when temperature is reduced to 77 K, the resistance reduces from $9.9\ \Omega$ to $8\ \Omega$. Another experiment that measured the resistance of metalization between measurement probe and contact pad (or between probe and solder pad) indicated that most of this D.C. connection resistance is contributed by the metalization between the probe and the contact pad. Thus we note that the contact between the switch beam and the probe pad is not affected by lowering the temperature of the switch to 77 K.

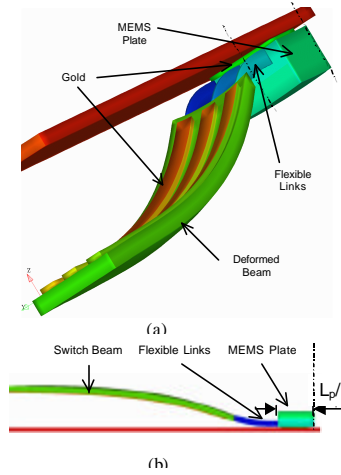


Fig. 3. Modified switch configuration and its simulated deformation at 77K: (a) 3-D solid model; (b) side view.

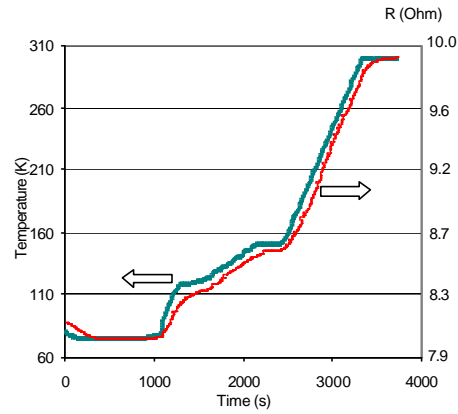


Fig. 4. D.C. connection resistance change with temperature.

III.4 RF Characterization

The solder height (Fig. III.1) determines the airgap between the top bias electrode and the CPW line. This airgap has substantial effect on the insertion loss. The measured insertion losses with different airgap heights are shown in Fig. III.5. As a result of this investigation, a $60\text{-}\mu\text{m}$ airgap is used in our current switch design. Insertion loss in this case is less than 0.8 dB up to 40 GHz.

When the switch is at down state, the scattering parameter values are measured at the temperature of 60 K and 300 K. Fig. III.6 demonstrates that the isolation values at 300 K and 60 K are almost identical, indicating that RF performance is not affected at cryogenic temperature. This isolation can be further improved by using LC resonance switching circuit design.

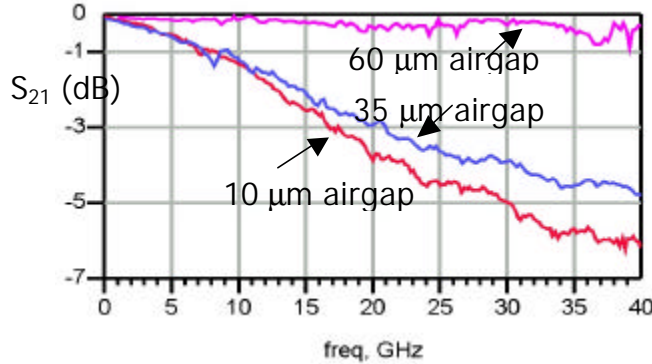


Fig. 5. Measured insertion loss of the switch with different air gap heights between the top electrode and CPW structure.

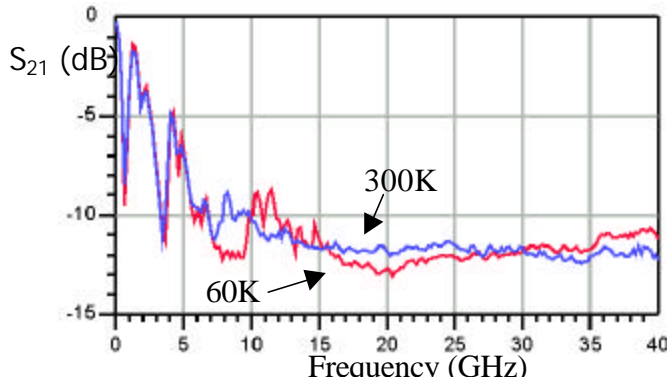


Fig. 6. Measured S_{21} magnitude values of the switch in down-state at 300 K and 60 K

As a conclusion, a novel RF MEMS switch fabricated by MUMPs process has been designed for the operation at cryogenic temperature. The electrical and mechanical models have been developed for optimizing the switch design. The measured switch shows a good insertion loss (<0.8 dB) up to 40 GHz. The difference of the insertion losses between the switch and the same length CPW line is less than 0.3 dB. The measured isolation values at both temperatures of 300 K and 60 K are both -12 dB at 20 GHz, showing the isolation is not affected by cryogenic temperature.

IV. Variable MEMS Capacitor for RF Applications

IV.1 Summary

As the flip-chip technology has become an accepted technology in the packaging community, the extension of this into the silicon MEMS world is a natural transition and thus has been further investigated. The work presented herein demonstrates the feasibility of integrating silicon MEMS with other substrates to create new systems, and/or devices. The flip-chip variable capacitor stands as an effective example of this. Alone, the device if left on the MUMPs low-resistance silicon substrate will not be a suitable device for RF applications due to severe losses. However, a transferred device to a more suitable substrate, such as alumina, without the presence of the MUMPs silicon substrate the RF performance is drastically increased.

Major stresses induced in the MEMS device due to thermal mismatch between the MEMS device and the substrate have been eliminated by design. And a linear relationship between capacitance and voltage has been obtained by the specific design of the variable MEMS capacitor. The measured Q-factor is over 200 at 1 GHz and the tuning ratio is approximately 3:1.

Furthermore, the great advantage of electrostatically actuated MEMS devices is that they can be designed with little current draw in mind, and generally do consume very low power. For the variable capacitor no current could be detected using an ammeter with 1 mA sensitivity, thus concluding that the power consumption of this device is very small to negligible.

IV.2 Introduction

RF components and modules are commonly fabricated and based on state-of the art devices using a combination of varactors, YIGs, FETs, GaAs or PIN diodes. Quite often these devices are used as tuning elements in Voltage-Controlled-Oscillators (VCOs) within receivers and transmitters. Varactors are commonly used for lower frequencies and YIG devices in the higher end of the microwave frequency band. YIG devices exhibit high Q-factors and a large tuning range, but have inherent problems such as relative large size, high power consumptions, and slow tuning speed. Varactors, on the other hand, are small in size, inexpensive and can easily be integrated into an existing circuit. However, some of the major drawbacks of varactors are the low Q-factor (at higher RF frequencies), limited tuning range and non-linear tuning (linearity) characteristics.

Recent efforts within the MEMS community have shown promising results in the development of a MEMS-based variable capacitor. Typically, these devices tune the capacitance by movement of micromachined electrodes by micro-electromechanical means. Since air is the common dielectric used (reducing the majority of dielectric losses), MEMS variable capacitors have on several occasions demonstrated huge improvements in Q-factor when compared to solid-state devices.

Regarding power requirements, it has been shown that MEMS devices can be designed to draw extremely small amounts of power when compared to for instance varactor devices. In a MEMS device there is no loss mechanism comparable to intrinsic semiconductor resistive losses or ferromagnetic material losses. This is especially true for electrostatically actuated devices where

the device virtually draws no current unless when tuning or being actuated, which is still very low. This is quite important for general communications systems, as well commercial and military applications, where increased functionality and reduced power consumption remain the elusive goal. Lastly, variable RF-MEMS capacitors have proven immune to drift in capacitance with RF power (linearity and harmonic production). That is, the capacitance does not change with varying power in the RF signal. It is believed, based on these merits, that variable RF-MEMS capacitors would be an excellent choice to replace current YIG and varactor devices in the next generation of micro receivers due to their small size and improved RF performance

IV.3 Results

The particular variable capacitor design investigated in this project consists of an array of individual capacitors. Each capacitor plate is of exactly the same surface area and the electrostatic force exerted on each plate is uniform throughout the device. A cascading snap-down effect is obtained by varying the stiffness of the individual support beams across the top-plate array. As the voltage between the two electrodes is increased, the top capacitor plates snap-down accordingly, as shown in Figure VI.1. This eliminates the highly non-linear CV relationship common to electrostatically actuated devices.

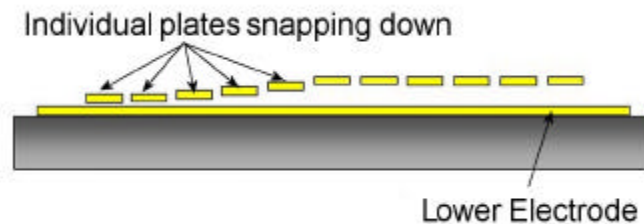


Figure VI.1: Side-view illustration of the cascading snap-down effect of the electrostatically actuated MEMS variable capacitor. The snap-down effect is obtained by varying the stiffness of the suspended beams across the top-plate array.

The flip-chip technique used to transfer the MEMS device to a receiving substrate allows complete removal of the host silicon substrate. By properly designing the device, the initial 3-layer MUMPs silicon surface micromachining is increased to a 5-layer process. In this design, the top electrode consists of the actual MEMS device and the lower electrode is constructed using the receiving substrate. The removal of the host silicon substrate is quite crucial for the RF performance of the device since the native substrate used in the MUMPs process is low-resistive silicon. If not removed, the presence of this substrate would degrade the RF performance and reduce the Q-factor. A cross-sectional view of the assembled capacitor is illustrated in IV.2. Figure IV.3 shows a photograph of an assembled version of the final design, where the individual fingers (capacitor plates) clearly can be seen.

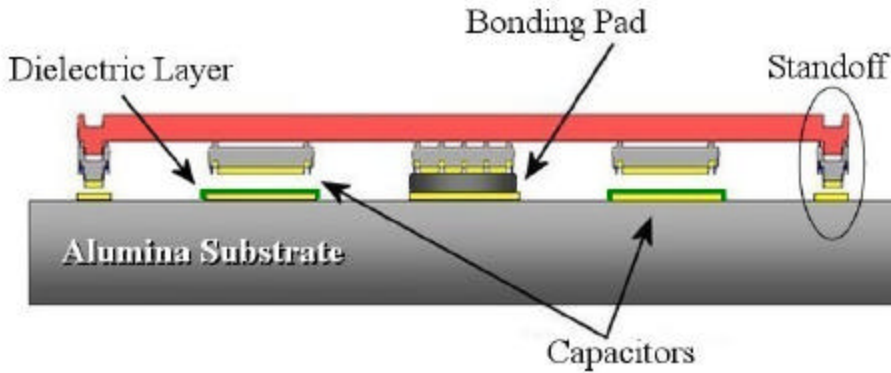


Figure IV.2: Illustration of improved fixed-free variable capacitor. This design utilizes only one bonding pad (down the centerline of the device) and underlying structures in the surface machining process to create standoffs at the end of each beam. This eliminates and reduces deformations occurring in the capacitor plates due to thermal mismatch between the receiving substrate and the top capacitor plates.

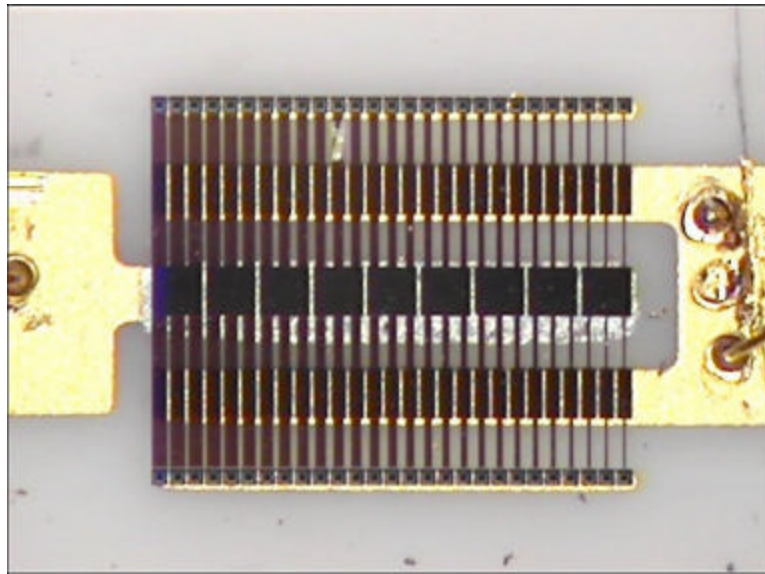


Figure IV.3: Photograph of variable MEMS capacitor. The individual top capacitor plates can clearly be seen in addition to the variation in flexure width connected to each top plate.

The CV relationship of the MEMS devices was tested using a LCR meter. The values obtained from the LCR meter were also later used to match RF measurements with lumped element models. Figure IV.4 shows the measured CV relationship for an 80-nm coated variable capacitor where the 60 plates give a practically continuous CV curve, despite the digital snap-down response of the actuation, due to the small difference in capacitance steps. The measured Q-factor for the MEMS variable capacitors exceeded our measurement circuit with a Q-factor around 240. Thus, the MEMS variable capacitor exhibits a Q-factor above 200 at 1 GHz.

To verify the actual LCR CV measurements and to investigate tuning at higher frequencies, the MEMS devices were mounted in a tunable end-coupled resonator as shown in Figure IV.5. Figure

IV.5 shows the tuning versus voltage of the resonator with 18.95% tuning at 2.375 GHz (center); 450 MHz from 2.6 GHz to 2.15 GHz. The actuation voltage is 0 - 55 V and the relative increase in loss with tuning is around 0.25 dB. This tuning is obtained without any measurable power consumption, and clearly illustrates the feasibility of using a variable MEMS capacitor as an active tuning element in an RF circuit.

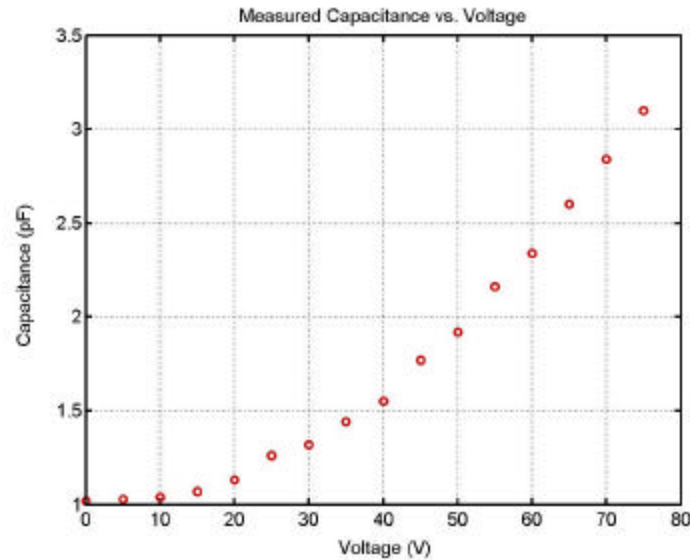


Figure IV.4: Measured capacitance versus voltage for the 80 nm coated MEMS device. Above a threshold voltage this C-V curve is linear, with a slope of 0.05pF/V.

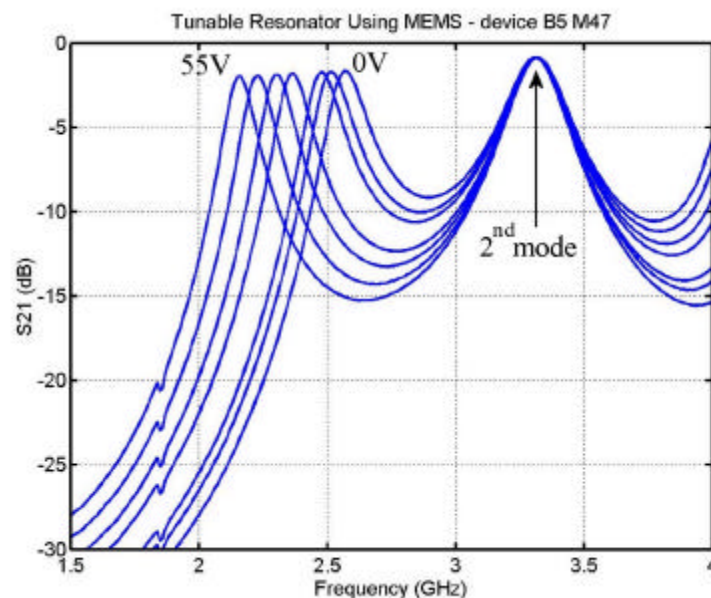


Figure IV.5: Measured tuning of resonance peak in improved resonator design. The resonator has 18.95% tuning at 2.375 GHz (center); 450 MHz from 2.60 GHz to 2.15 GHz at 0 - 55 V. Note how flat the resonant peaks remain while tuning, contributed to a high Q-factor in the MEMS device. The relative capacitance change of the MEMS device is from 0.48 - 1.3 pF.

V. Reflection-type MEMS Variable-Capacitor Phase Shifters

V.1 Summary

Phase shifters using MEMS switches and distributed MEMS transmission line have been reported in literature. However, the phase shifter using two MEMS capacitors has not been reported so far. In this part of the project, we report, for the first time, the development of an 180° reflection-type phase shifter using two MEMS variable capacitors. The variable capacitors used in the phase shifter are based on the variable capacitors developed in our group in this project and characterized around 1 GHz. The capacitor design is modified for operation at 26.5 GHz for phase shifter application. The measured capacitance varies from 0.1 pF to 0.37 pF when an actuation voltage of 60 volts is applied. A new tether-MEMS transfer technology for MUMPs process is developed and used to transfer the two capacitors onto the phase shifter circuit. As another component in the reflection-type phase shifter, CPW hybrid operating at 26.5 GHz is designed and measured. Experimental results yield a phase shift of 179.3° at 26.5 GHz for this phase shifter using two MEMS capacitors. We achieved a good agreement between the measured and designed relative phase shift.

V.2 Introduction

Phase shifters using MEMS switches and distributed MEMS transmission line have been reported in literature. However, the phase shifter using two MEMS capacitor has not been reported so far. In this part of the project, we report, for the first time, the development of an 180° phase shifter using two MEMS variable capacitors. The MEMS capacitor used in phase shifter is based on our digitally-controllable variable capacitor developed in this project. A newly developed technology, Atomic Layer Deposition (ALD) for MEMS applications is used to deposit a thin layer of Alumina for insulation.

The basic structure of the reflection-type phase shifter is shown in Fig. V.1. This basic hybrid-coupled reflection-type phase shifter consists of three elements: a 3-dB quadrature hybrid, and two identical phase shifting circuits, as in Fig. V.2.

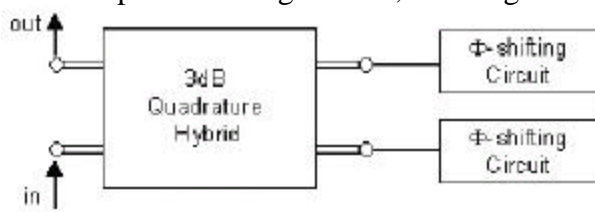


Fig. V.1. Architecture of a reflection-type phase shifter. (The two MEMS variable capacitors are included in Φ -shifting circuits.)

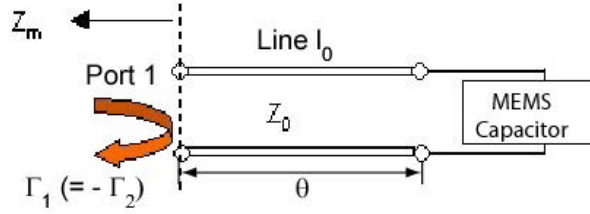


Fig. V.2. Structure of phase-shifting circuits.

V.3 Measurements

A. MEMS variable capacitors for operation at 26.5 GHz

The digitally controllable variable capacitor developed in our group in this project has been modified characterized for operation at 26.5 GHz. One of the capacitor mounted in CPW shunt configuration is shown in Fig. V.3. The capacitor is actuated using electrostatic force by applying a voltage from 0 to 60 volts. This capacitor is tested separately. The measured capacitance varies from 0.1 pF in up-state to 0.37 pF in down-state as shown in Fig. V.4.

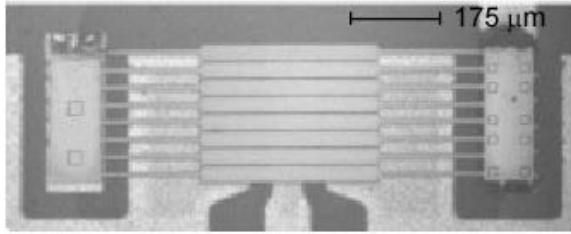


Fig. V.3. Photo of digitally controllable variable capacitor mounted on CPW for operation at 26.5 GHz.

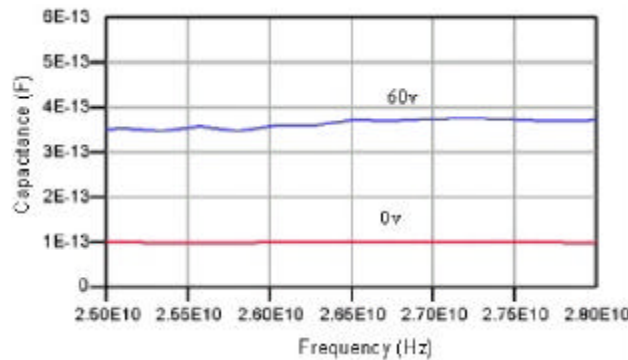


Fig. V.4. Measured capacitance values when the actuation voltage of 0 and 60 volts are applied.

B. CPW Branchline Hybrids: Design And Optimization

Another important component of the reflection-type phase shifter shown in Fig. V.1 is the 3-dB quadrature hybrid. The hybrid circuit is fabricated and measured separately. The test structure layout is shown in Fig. V.5. The two ports at the left-hand side are open and the VNA measurement is taken on the two ports at the right-hand side. The two identical hybrid circuits are fabricated and measured. The additional impedance transformers are deembedded from the measurement results

and the reference planes are shifted to the dotted lines shown in Fig. V.5. The deembedded branch-line hybrid S_{21} magnitude values are plotted in Fig. V.6. We note that the insertion loss is about 0.7 dB. The slight difference of the two insertion loss curves is due to the tolerances in the fabrication, especially the wire bonding.

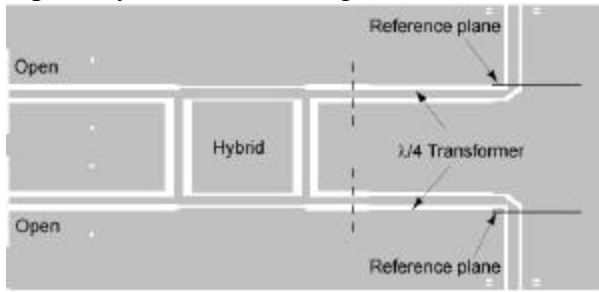


Fig. V.5. Layout of the hybrid test structure with the two hybrid ports on the left-hand side open.

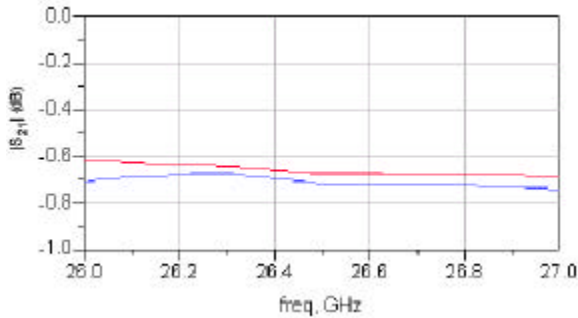


Fig. V.6. Measured insertion losses of the two identical hybrids with the dotted lines in Fig. 5 as reference planes.

C. Characterization of 180° Reflection-Type Phase Shifter

The complete 180° phase shifter layout is shown in Fig. V.7. The MEMS capacitors are bonded on the left hand side of the figure with the DC bias line extended to the left. A photo of 180° phase shifter for VNA measurement is shown in Fig. V.8. The measurement reference planes are shown in Fig. V.7 as solid lines. The impedance transformers are deembedded from the measured S-parameters. The dotted lines in Fig. V.7 show the reference planes for the S-parameters in Figs. V.9, V.10 and V.11. The multi-line TRL procedure developed at NIST laboratories is used for on-wafer calibration.

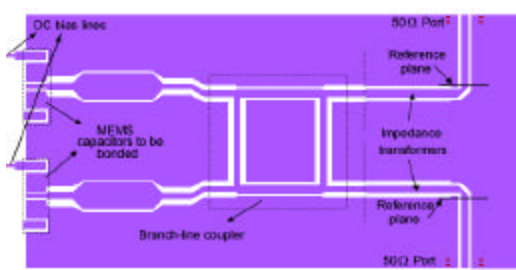


Fig. V.7. Layout of 180° phase shifter measurement.

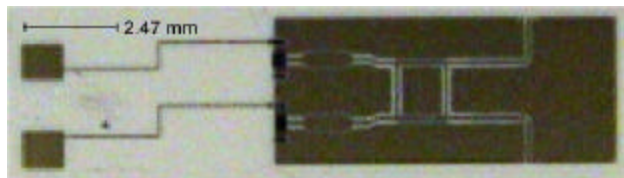


Fig. V.8. Photo of 180° phase shifter for VNA for VNA measurement before bonding wires are added.

The measured relative phase shift (Fig. V.9) is 179.30° at 26.5 GHz when a 55-Volt bias is applied on both MEMS capacitors at the same time. This phase-shift value is fairly constant ($177.72^\circ \pm 5.04^\circ$) over the frequency range of 26--27 GHz. The insertion loss (Fig. V.10) at 26.5 GHz is 3.0 dB at 0 volt and 3.76 dB at 55 volts. These values are better (2.84 dB at 0 volts and 3.36 dB at 55 volts) at 26 GHz, and slightly worse (3.69 dB at 0 volt and 3.91 dB at 55 volts) at 27 GHz. This is consistent with the general trend of losses increasing with frequency. The return loss (Fig. V.11) at 26.5 GHz is 22 dB at one state and 25 dB at the other state. Over the frequency range of 26 to 27 GHz, return loss values are better than 13 dB. The minimum seen in the return loss curve is caused by the fact that the hybrid, $\lambda/4$ transformers, and phase shifting circuit have been designed at a single design frequency. We have achieved a good agreement between measured and design values of phase shift.

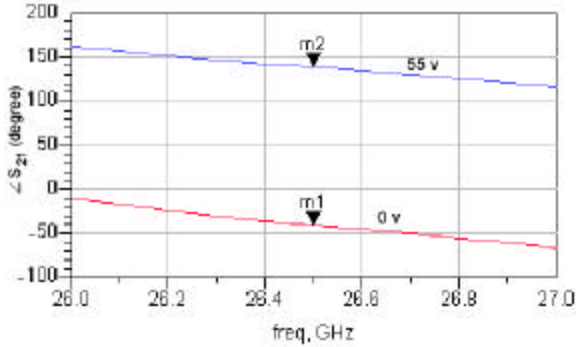


Fig. V.9. Measured S_{21} phase of 180° phase shifter at 0 and 55 volts

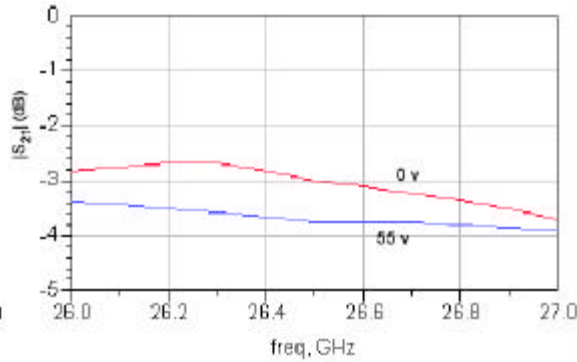


Fig. V.10. Measured S_{21} magnitude of 180° phase shifter at 0 and 55 volts (reference planes shown as the dotted lines in Fig. V.7).

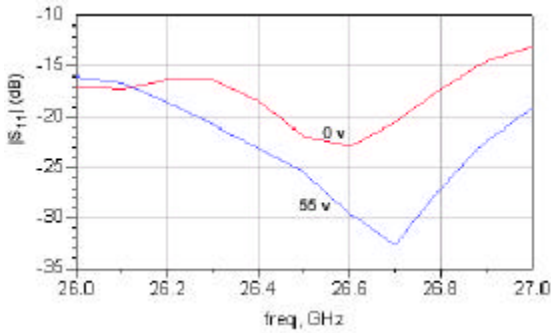


Fig. V.11. Measured S_{11} magnitude of 180° phase shifter at 0 and 55 volts (reference planes shown as the dotted lines in Fig. 7).

As a conclusion, we have developed a phase shifter for operation at 26.5 using two MEMS variable capacitors as phase shifting devices. The MEMS variable capacitors are developed in this project. The design optimization of coplanar branchline hybrid used has been discussed. The experimental results have shown a phase shift of 179.30° at 26.5 GHz. We achieved a good agreement between the measured and designed relative phase shift.

VI. Administration

VI.1 Personnel

Investigators

Dr. Y. C. Lee, Principal Investigator
Dr. K. C. Gupta, Co-Principal Investigator
Dr. Victor M. Bright, Co-Principal Investigator

Graduate Students

Mr. Bingzhi Su (Ph.D. 2000)
Capt. M. Adrian Michalick (Ph.D. 2001)
Ms. Zhiping Feng (Ph.D. 2000)
Mr. Huan-Tong Zhang (Ph.D. 2002)
Mr. Nils Hoivik (Ph.D. 2002)
Mr. Faheem Faheem (Ph.D. student)
Mr. Alexander Laws (Ph.D. student)

Professional Research Assistants

Mr. Wenge Zhang
Ms. Ann Geesaman

VI.2 Awards, Patents, Publications or Presentations Fully or Partially Supported

Awards

1. Best Student Paper, "Mechanical and electrical design of a novel RF MEMS switch for cryogenic applications" in 35th International Symposium on Microelectronics, Denver, CO, September 4-6, 2002.
2. Honorable Mention, Patrick Bell, Nils Hoivik, Victor Bright, Zoya Popovic, "*A Frequency Tunable Half-Wave Resonator Using a MEMS Variable Capacitor*", in 35th International Symposium on Microelectronics, Denver, CO, September 4-6, 2002.

Patent (pending):

1. "Atomic Layer Deposition on Micro-Mechanical Devices," V. Bright, J. Elam, F. Fabreguette, S. George, N. Hoivik, Y. C. Lee, R. Linderman, M. Tripp, U. S. Patent Pending, filed on December 17, 2002.

Keynote speeches:

1. "Packaging for MEMS," Y. C. Lee, Keynote Speech, International Symposia on Materials Science for the 21st Century, Symposium E: Micromaterials - New Frontier for the 21st Century, Osaka, Japan, May 21-26, 2001.

2. "Teaching and Research for MEMS Design and Packaging," Y. C. Lee, Keynote speech (without paper), Chinese Society of Mechanical Engineers' Annual Meeting, Taipei, Taiwan, December 6-7, 2001.
3. "Thermo-mechanical Design for MEMS and Packaging," Y. C. Lee, Keynote speech, The 25th Conference on Theoretical and Application Mechanics, Taichung, Taiwan, R. O. C., December 15-16, 2001.
4. "Transport Phenomena and Microelectromechanical Systems (MEMS)," keynote speech, Y. C. Lee, International Heat Transfer Conference, Grenoble, France, August 19-23, 2002.

Publications

1. "Flip-Chip Assembly for Si-Based RF MEMS" K. F. Harsh, W. Zhang, V. M. Bright, and Y. C. Lee, IEEE MEMS '99, Orlando, January 17-21, 1999.
2. "Flip-chip assembly for RF and optical MEMS," W. Zhang, K.F. Harsh, M.A. Michalick, V.M. Bright, and Y.C. Lee, *The ASME International, Intersociety Electronic & Photonic Packaging Conference & Exhibition (InterPACK'99)*, Maui, Hawaii, June 13-19, EEP-Vol. 26-1, Advances in Electronic Packaging, pp. 349-354, 1999.
3. "Design and Modeling of RF MEMD Tunable Capacitors Using Electro-Thermal Actuators," Z. Feng, W. Zhang, B.S. Su, K. Marsh, K.C. Gupta, V. Bright, and Y.C. Lee, The 1999 IEEE MTT-S International Microwave Symposium, June 12 - 19, 1999; Anaheim, California, USA
4. "The Realization and Design Considerations of a Flip-Chip Integrated MEMS Tunable Capacitor," K. Harsh, B. Su, Wenge Zhang, Victor M. Bright and Y. C. Lee, *Sensors and Actuators A*, Vol. 80, pp. 108-118, 2000.
5. "MEMS-based Variable Capacitor for Millimeter-wave Applications," Y. C. Lee, Zhiping Feng, Huantong Zhang, Wenge Zhang, Bingzhi Su, K. C. Gupta and Victor M. Bright, the 2000 *Solid-State Sensor and Actuator Workshop*, June 4-8, 2000, Hilton Head Island, SC.
6. "Optical and RF MEMS Devices for Electronics Circuits," Y. C. Lee, V. M. Bright and K. C. Gupta, International Conference on High-Density Interconnect and Systems Packaging, Denver, April 25-28, 2000.
7. "MEMS-Based Variable Capacitor for Millimeter-wave Applications," Zhiping Feng, Huantong Zhang, Wenge Zhang, Bingzhi Su, K. C. Gupta, Victor M. Bright, and Y. C. Lee, *Sensors and Actuators A*, Vol. 91, pp. 256-265, 2001.
8. "Digitally Controllable Variable High-Q MEMS Capacitor for RF Applications", N. Hoivik, A. Michalick, Y.C. Lee, K.C. Gupta and V.M. Bright, IEEE MTT-S 2001 International Microwave Symposium, Phoenix (Arizona), May 20-25, 2001, Symposium Digest, pp 2115-2118.
9. "Flip-Chip Variable High-Q MEMS Capacitor for RF Applications", Nils Hoivik, Yung-Chen Lee and Victor M. Bright, Proceedings of IPACK'01, The Pacific RIM/ASME International Electronic Packaging Technical Conference and Exhibition, July 8-13, 2001, Kauai, Hawaii, USA.

10. "A Frequency Tunable Half-Wave Resonator Using a MEMS Variable Capacitor", Patrick Bell, Nils Hoivik, Victor Bright, Zoya Popovic, Proceedings of 2002 IMAPS conference, Denver CO, September 2002, pp 377-382.
11. "Atomic Layer Deposition of Conformal Dielectric and Protective Coatings for Released Micro-Electromechanical Devices", N. Hoivik, J. W. Elam, R. Linderman, V. M. Bright, S. M. George and Y.C. Lee , IEEE Int'l. MEMS2002 Conference at Las Vegas, Jan. 20-24, 2002. Technical Digest, pp. 455-458.
12. "Atomic Layer Deposition (ALD) Technology for Reliable RF MEMS", N. Hoivik, J. W. Elam, S. M. George, K.C. Gupta, V. M. Bright and Y.C. Lee, IEEE MTT-S 2002 International Microwave Symposium, Seattle WA, June 02-07, 2002, Symposium Digest, pp 1229-1232.
13. "MEMS variable capacitor phase shifters: Part I – loaded-line phase shifter", H. Zhang, A. Laws, K.C. Gupta, Y.C. Lee and V.M. Bright, accepted for publication in International Journal of RF and Microwave Computer-Aided Engineering, June 2003.
14. "MEMS variable capacitor phase shifters: Part II – reflection-type phase shifter", H. Zhang, A. Laws, K.C. Gupta, Y.C. Lee and V.M. Bright, accepted for publication in International Journal of RF and Microwave Computer-Aided Engineering, June 2003.
15. "Mechanical and electrical design of a novel RF MEMS switch for cryogenic applications", H. Zhang, Victor M. Bright, Y.C. Lee and K.C. Gupta, Proceedings of the 35th International Symposium on Microelectronics, Denver, CO, September 4-6, 2002.
16. "Post-Enabled Flip-Chip Assembly for Manufacturable RF-MEMS," F. Faheem, Y.C. Lee, K.C. Gupta, Transducer03, Boston, July, 2003
17. "Post-Enabled Precision Flip-Chip Assembly for Variable MEMS Capacitor," F. Faheem, N. Hoivik, Y.C. Lee , K.C. Gupta, Microwave Symposium Digest, 2003 IEEE MTT-S International, Baltimore, PA, June, 2003.
18. "Atomic Layer Deposited Protective Coatings for Micro-Electromechanical Systems" Nils Hoivik, Jeffrey Elam, Ryan Linderman, Victor M. Bright, Steven George and Y.C. Lee, accepted for publication in Sensors and Actuators, A: Physical, 2003
19. "A Frequency Tunable Half-Wave Resonator Using a MEMS Variable Capacitor", Patrick Bell, Nils Hoivik, Victor Bright, Zoya Popovic, invited paper to the Microelectronics International, 2003.
20. "Design, Packaging and Reliability of Foundry-Based RF MEMS," N. Hoivik, F. Faheem, H. S. Park, F. H. Fabreguette, K. C. Gupta, V. M. Bright, S. M. George and Y.C. Lee, Government Microcircuit Applications and Critical Technology Conference (GOMAC), Tampa, FL, March 31- April 3, 2003.